ChemComm
Chemical Communications

Accepted Manuscript

This article can be cited before page numbers have been issued, to do this please use: F. Gang, H. Yan, C. Ma, L. Jiang, Y. Gu, Z. Liu, L. Zhao, X. Wang, J. Zhang and X. Sun, *Chem. Commun.*, 2019, DOI: 10.1039/C9CC04241E.

ROYAL SOCIETY OF CHEMISTRY

rsc.li/chemcomm

View Article Online
DOI: 10.1039/C9CC04241E

COMMUNICATION

Robust magnetic double-network hydrogels with self-healing, MR imaging, cytocompatibility and 3D printability

Received 00th January 20xx,
Accepted 00th January 20xx

DOI: 10.1039/x0xx00000x

Fangli Gang,[a,b] Hao Yan,[d] Chunyang Ma,[b] Le Jiang,[b] Yingying Gu,[e] Ziyu Liu,[e] Lingyun Zhao,[b,c] Xiumei Wang,[b,c] Jiwen Zhang,*[a] and Xiaodan Sun*[b,c]

Herein, we have fabricated a novel robust self-healing magnetic double-network hydrogel by multiple interactions between bondable magnetic Fe_3O_4 and chitosan-polyolefin matrix, and the hydrogel also exhibits excellent magnetogenic effect and MR imageability. The practical potential of the magnetic double-network hydrogel is further revealed by their 3D-printing performance.

Functional composite material made of nanoparticles with unique optical, electrical and magnetic properties and hydrogels can realize the functions of image monitoring, controlled drug release and multi-modal combination therapy, after implantation *in vivo*.[1-8] Therefore, they have attracted wide attention in the field of biomedicine. In recent years, magnetic hydrogels, which are composed of magnetic particles and hydrogel matrix, have developed rapidly because of their promising applications in drug release,[9-11] actuators,[12, 13] photonic crystals[14, 15] and biomedical engineering.[16, 17] Despite extensive research into the development of magnetic hydrogels, only a few studies have attempted to capture other functional properties, such as high mechanical strength and self-healing. The development of magnetic hydrogels with self-healing and high mechanical strength is of great significance for the development of biomedical fields such as tissue engineering, cancer treatment and medical device.

Double network (DN) hydrogels are emerging to enhance the mechanical performance of conventional hydrogels due to its rigid-flexible structure resembling collagen-proteoglycans in the extracellular matrix, which can effectively dissipate energy.[18-21] The general method of preparing robust magnetic DN hydrogels is to physically disperse magnetic particles (Fe_2O_3, Fe_3O_4) in the hydrogel matrix, resulting in uneven network structure and poor mechanical properties, due to the easy agglomeration of the nano-filler particles.[22-24] Furthermore, magnetic hydrogels with high strength usually do not have good self-healing[25, 26] and compatibility. Therefore, designing a magnetic hydrogel with multiple functions remains a big challenge.

Herein, we report a novel robust magnetic nano-Fe_3O_4 composite polyolefin-chitosan (AAD-CS-Fe) double network hydrogel with multiple functions (Scheme 1). Fe_3O_4 nanoparticles about 40~50 nm synthesized following an improved solvothermal method[27] (Fig. S1) have relatively few surface groups and have been proven very suitable for in situ surface coating and in situ reaction.[28, 29] Then, magnetic nano-Fe_3O_4 was treated with HCl solution (pH≈1) to expose more Fe ions as bonding sites (Scheme 1a), and coordinated with different carboxyl group/hydroxy group in AAD terpolymer, thus improving the dispersion of magnetic particles in hydrogels (Fig. S2). Subsequently, one-step amidation reaction of acryloyl chloride with dopamine hydrochloride gives a dopamine acrylamide (DAm) for the synthesis of a polyolefin polymer chain (Scheme 1b), with the aim of increasing the cell affinity of the hard hydrogel. Finally, AA, AM and DAm monomers were chemically polymerized by APS in the presence of chitosan and nano-Fe_3O_4, to form a physically and chemically crosslinked polyolefin-chitosan double network hydrogel (Scheme 1c). The synthesized hydrogels were immersed in saturated NaCl solution to increase the physical entanglement between chitosan molecular chains by forming intermolecular aggregation, which further enhances the mechanical properties of the hydrogels.[30]

Taking advantages of rigid-flexible coordinated DN architecture and synergistic effect including the coordination of Fe ion on the surface of the nanoparticle with the carboxyl group/hydroxyl group, hydrogen bonds and π-π stacking, the AAD-CS-Fe DN hydrogel exhibited uniform porous network

[a] College of Chemistry & Pharmacy, Shaanxi Key Laboratory of Natural Products & Chemical Biology, Northwest A&F University, Yangling, Shaanxi, 712100, China
[b] State Key Laboratory of New Ceramics and Fine Processing, School of Materials Science and Engineering, Tsinghua University, Beijing,100084, China.
[c] Key Laboratory of Advanced Materials of Ministry of Education of China, School of Materials Science and Engineering, Tsinghua University, Beijing 100084, China.
[d] Harvard Medical School and Wellman Center for Photomedicine, Massachusetts General Hospital, 50 Blossom Street, Boston, MA 02114, USA.
[e] Division of Surgery and Interventional Science, University College London, Gower Street, London, UK.

†Electronic Supplementary Information (ESI) available: Experimental procedures and supporting figures. See DOI: 10.1039/x0xx00000x

DOI: 10.1039/C9CC04241E

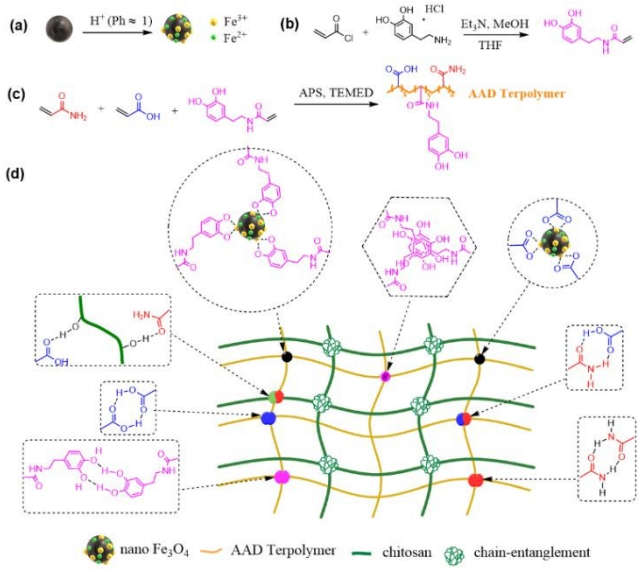

Scheme 1 Schematic strategy of the design of nano-Fe_3O_4 composite double-network hydrogels. Chemical synthesis of a) hydrochloric acid etched nano-Fe_3O_4; b) DAm; c) AAD terpolymer. d) Illustration of nanocomposite DN hydrogel. Hydrogen bonds were displayed in rectangular dashed boxes, while ions coordination in circular dotted box and π-π stacking in hexagonal dotted box.

structure (Fig. 1a), excellent mechanical properties (Fig. 1b-1e) and self-healing properties (Fig. 1f). To investigate the mechanical properties of the AAD-CS-Fe DN hydrogel, a series of control hydrogels were prepared (Table S1). As shown in Fig. 1b and 1d, the first six DN hydrogel exhibited a compressive strength of 0.38 to 2.23 MPa, a tensile strength of 54.02 to 421.77 KPa, and a compressive modulus of 0.24 to 2.51 MPa, which is much higher than that of a SN hydrogel (0.24 MPa, 39.27 KPa, 0.11 MPa). Similarly, the comparison of the storage modulus (G′) in Figure 1c showed that the SN hydrogel was less rigid than all DN hydrogels. However, due to the absence of a rigid network, a SN hydrogel containing only a flexible network exhibited a greater tensile elongation (234.23%) and a higher swelling ratio (5.89 g/g). Subsequently, considering the addition of different iron contents will also affect the mechanical properties of the hydrogel, we set up several control groups to verify the effect of iron on the performance of hydrogel, including AAD-CS without any Fe, AAD-CS-Fe^{3+} containing Fe^{3+}, AAD-CS-nano containing nano-iron oxide particles and AAD-CS-Fe containing HCl-treated nano-Fe_3O_4. As can be seen from Fig. 1b and 1c, the compressive strength, compressive modulus and G′ are both AAD-CS-Fe > AAD-CS-Fe^{3+}> AAD-CS-nano > AAD-CS, indicating that the increase of DN hydrogel strength is due to the synergistic effect of coordination of Fe ions exposed on the surface of nanoparticles and nanoparticles themselves. In addition, the strength of AAD-CS-Fe hydrogel can be adjusted to a large extent (0.25 MPa to 2.29 MPa) by changing the filling amount of nano-Fe_3O_4 particles and the ratio of other components (Fig. S3). Furthermore, in this work, the self-healing of the robust magnetic hydrogels is attributed to multiple dynamic ions coordination bonds between carboxyl or hydroxyl groups and Fe ions on the surface of nanoparticles, and hydrogen bonds between various groups (Scheme 1d). As illustrated in Fig. 1f, the hydrogel was cut into four pieces and immediately re-contacted at 70 °C. After contact for 12 h, the healed gel had no obvious cuts and can bear stretching without breaking.

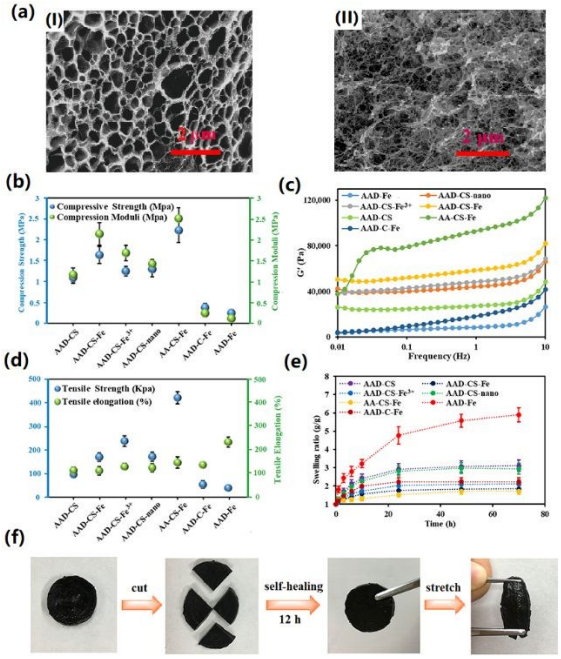

Fig. 1 Characterization of the hydrogels. a) SEM images of the internal microstructures of the hydrogels at different concentrations of Fe_3O_4 nanoparticles in water. I) 0 mg·mL^{-1}; II) 16 mg·mL^{-1}. b) Compressive strength and compressive moduli of different hydrogels. c) The storage modulus (G′) of different hydrogels in the frequency range of 0.01 to 10 Hz at 1.0% strain amplitude. d) Tensile strength and tensile elongation of different hydrogels. e) Swelling ratio (g/g) of various hydrogels at different time points in PBS. f) Self-healing properties of AAD-CS-Fe DN hydrogel.

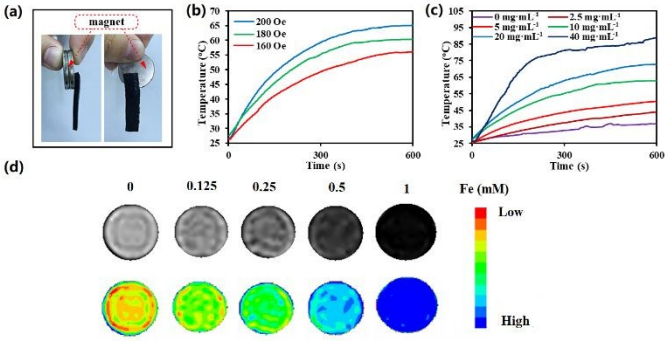

Fig.2 Magnetothermal properties and imageability of AAD-CS-Fe DN hydrogel containing 16 mg/mL nano-Fe_3O_4. a) Macroscopic picture of the magnetic hydrogel under the attraction of a magnet. b) Heat-induction properties of 0.25 g Fe_3O_4-based magnetic hydrogels (8 mg/mL Fe_3O_4) in 0.5 mL H_2O under AMF with different intensities after 600 s. c) Heat-induction properties of DN hydrogels with different Fe concentration under AMF. d) T2-weighted MR images of hydrogels with different concentrations of nano-Fe_3O_4.

This ionic coordination on the surface of magnetic nano-Fe_3O_4 synergized with hydrogen bonds and π-π stacking significantly improved the mechanical properties, self-healing and anti-swelling ability of the composite hydrogel, while

keeping the excellent magnetocaloric effect and MR imaging of hydrogels entrusted by nano-Fe_3O_4 (Fig. 2). The magnetic properties of DN hydrogels are also attributed to the addition of 50 nm diameter paramagnetic nano-Fe_3O_4 (Fig. 2a), and its inductive thermal properties depend on the nano-Fe_3O_4 dopants at a certain AMF (282 kHz, 180 Oe), generally showing a dose dependency (Figure 2b). Moreover, the hydrogel exhibited enhanced heating ability at higher intensity AMF (Figure 2c). The hydrogel with heat-induction property may be used in the treatment of tumors and drug-controlled release.[27, 28] Furthermore, the imageable function of the hydrogel also provides the possibility of "theranostics" after implanting in the body. As can be seen from the Fig. 2d, the signal enhancement of the T2-weighted MR image of the hydrogel increases with increasing Fe_3O_4 content.

In general, most of reported hard hydrogels have poor cell affinity and are not conducive to cell adhesion and growth. Therefore, the addition of propylene dopamine (DAm) monomer (Scheme 1b) to a robust magnetic DN hydrogel can effectively improve its cell affinity (Fig. 3). The ability of the hydrogels to interact with cells was assessed by culturing L929 fibroblasts on the surface of prepared hydrogels. Representative confocal laser scanning microscopy (CLSM) of LIVE/DEAD assay and SEM images showed more living cells on the AAD-Fe and AAD-CS-Fe hydrogels than AA-CS-Fe hydrogel, indicating that the addition of adhesion-promoting DAm in the hydrogels facilitated cells-gels favorable interaction. In addition, the fibroblasts adhered and spread more after CS and nano-Fe_3O_4 incorporation, which indicated that formation of DN hydrogels enhanced the cell affinity of hydrogels. Further quantitative evaluation of cell proliferation on hydrogels after 3 and 5 days of culture using CCK-8 assay was shown in Fig. 3g. After 3 days of culture, the DAm-containing hydrogels had higher cell viability as compared to the DAm-free ones, evidenced by a greater number of living cells in Fig. 3g, indicating that DAm promoted cell proliferation during the initial stage. After 5 d of incubation, L929 cells proliferated on all hydrogels, and DAm-containing nanocomposite DN hydrogels have higher cell viability than other component hydrogels. These results indicated that DAm, nano-Fe_3O_4 and double network structures played a key role in promoting cell adhesion and proliferation on the hydrogels.

The personalized customization of hydrogels or the construction of complex anatomical structures through 3D printing can further reveal the practical application potential of robust magnetic hydrogels in biomedical fields.[33-37] However, the printing of hydrogels is often limited by the inability to form quickly after extrusion, so the approach we take was to print the gel in a pre-solution of a saturated sodium chloride solution containing APS. A video (Movie S1) of DN hydrogel printing was provided in the Supporting Information. The 3D printing process was as follows: in the first step, the AAD-CS-Fe DN hydrogel containing 8 mg/mL nano-Fe_3O_4 precursor without APS was prepared in the needle tube. Afterwards, a saturated sodium

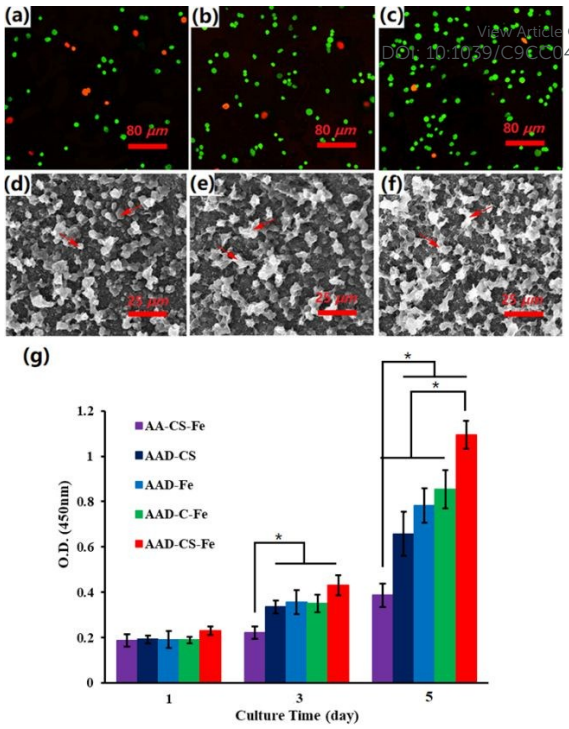

Fig.3 Cytocompatibility of the various hydrogels. Representative CLSM images of LIVE/DEAD assay and SEM images of L929 on a, d) AA-CS-Fe hydrogel; b, e) AAD-Fe hydrogel; and c, f) AAD-CS-Fe hydrogel. g) Cell proliferation on hydrogels after 1, 3 and 5 days of culture. * represents statistical significance ($p < 0.05$).

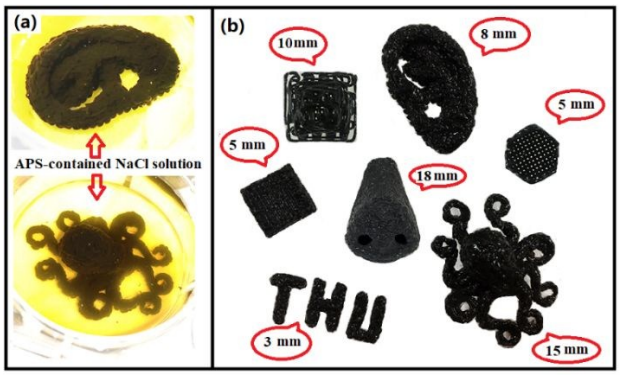

Fig. 4 3D Printing preparation and characterization of AAD-CS-Fe DN hydrogel containing 8 mg/mL nano-Fe_3O_4. a) 3D model of the DN hydrogel in the pre-solution just after printing. b) 3D printed various shapes. Quadrangular pyramid, left ear, hexagonal prism, cuboid, nose, letters, octopus (from left to right, from top to bottom). The height of the corresponding models is shown in the red box.

chloride solution containing APS was prepared as a pre-solution to receive the gel. After printing, the models were stabilized in the pre-solution for several hours and rinsed with deionized water. Fig. 4 demonstrates the various custom shapes of the 3D printed DN hydrogel. Quadrangular pyramid and hexagonal prism presented printing of objects or scaffolds with uniform holes. Cuboid and letters showed printing of objects with high vertical aspect ratios. Left ear, nose and octopus demonstrated the ability to print complex structures with overhangs and high vertical aspect ratios. 3D printing is often used in biomedical

applications to print anatomical complex structures that are not cut by scalpels. In order to be used *in vivo*, the printed hydrogel scaffold should not lose its shape and strength after being soaked in water for a long time. In Fig. 4b, there was no obvious change in the morphology of DN hydrogels in the deionized water for 24 h.

In summary, a combination of chitosan-polyolefin double network hydrogel and bondable magnetic nano-Fe_3O_4 were employed to meet the excellent mechanical properties, self-healing and cytocompatibility of magnetic hydrogel. Fe ions are exposed as bonding sites on the surface of magnetic Fe_3O_4 etched by HCl to ionic coordinate with different carboxyl groups/hydroxy groups, which increased the dispersion of Fe_3O_4 in hydrogels. This ionic coordination synergized with hydrogen bonds and π-π stacking to improve the mechanical properties, self-healing and anti-swelling ability of magnetic DN hydrogels, while keeping the excellent magnetocaloric effect and MR imaging of hydrogels entrusted by nano-Fe_3O_4. Moreover, the dopamine acrylamide (DAm) monomer in the AAD triblock copolymer gives the hydrogel better cell affinity and self-healing. Changes in the Fe_3O_4 content and composition ratio leads to the controllability of the hydrogel strength with good cytocompatibility. Notably, to demonstrate the potential of the robust magnetic hydrogel implantation in vivo, several 3D printing anatomical structures was constructed. Considering the magnetism performance pairing with high-strength (>2 MPa), self-healing, cytocompatibility, MR imaging and 3D printability, the developed hydrogel offers superior functionalities than previously reported.

This work was supported by Intergovernmental cooperation in science and technology [2016YFE0125300]; the National Key Research and Development Program of China [2016YFB0700802]; Major projects of the National Social Science Funding (17ZDA019); the National Natural Science Foundation of China (81671829); Tsinghua University Initiative Scientific Research Program (2017THZWYX07).

Conflicts of interest

There are no conflicts to declare.

Notes and references

1. Y. Wu, H. Wang, F. Gao, Z. Xu, F. Dai and W. Liu, *Adv. Funct. Mater.*, 2018, **28**, 1801000.
2. F. Gao, W. Xie, Y. Miao, D. Wang, Z. Guo, A. Ghosal, Y. Li, Y. Wei, S. S. Feng, L. Zhao and H. M. Fan, *Adv. Healthc. Mater.*, 2019, **8**, 1900203.
3. G. He, S. Chen, Y. Xu, Z. Miao, Y. Ma, H. Qian, Y. Lu and Z. Zha, *Mater. Horiz.*, 2019, **6**, 711-716.
4. H. Ruan, Q. Hu, D. Wen, Q. Chen, G. Chen, Y. Lu, J. Wang, H. Cheng, W. Lu and Z. Gu, *Adv. Mater.*, 2019, **31**, 1806957.
5. H. Wu, L. Song, L. Chen, W. Zhang, Y. Chen, F. Zang, H. Chen, M. Ma, N. Gu and Y. Zhang, *Acta Biomater.*, 2018, **74**, 302-311.
6. Z. Jin, K. Wu, J. Hou, K. Yu, Y. Shen and S. Guo, *Biomaterials*, 2018, **153**, 49-58.
7. J. Song, W. He, H. Shen, Z. Zhou, M. Li, P. Su and Y. Yang, *Chem. Commun.*, 2019, **55**, 2449-2452.
8. M. L. Xu, L. Y. Guan, S. K. Li, L. Chen and Z. Chen, *Chem. Commun.*, 2019, **55**, 5359-5362.
9. N. S. Satarkar and J. Z. Hilt, *J. Control. Release*, 2008, **130**, 246-251.
10. K. Hu, J. Sun, Z. Guo, P. Wang, Q. Chen, M. Ma and N. Gu, *Adv. Mater.*, 2015, **27**, 2507-2514.
11. X. Zhao, J. Kim, C. A. Cezar, N. Huebsch, K. Lee, K. Bouhadir and D. J. Mooney, *Proc. Natl. Acad. Sci. U S A*, 2011, **108**, 67-72.
12. Y. S. Kim, M. Liu, Y. Ishida, Y. Ebina, M. Osada, T. Sasaki, T. Hikima, M. Takata and T. Aida, *Nat. Mater.*, 2015, **14**, 1002-1007.
13. M. M. Schmauch, S. R. Mishra, B. A. Evans, O. D. Velev and J. B. Tracy, *ACS Appl. Mater. Inter.*, 2017, **9**, 11895-11901.
14. J. Ge and Y. Yin, *Angew. Chem. Int. Ed. Engl.*, 2011, **50**, 1492-1522.
15. H. Hu, C. Chen and Q. Chen, *J. Mater. Chem. C*, 2013, **1**, 6013-6030.
16. J. I. Kim, C. Chun, B. Kim, J. M. Hong, J. K. Cho, S. H. Lee and S. C. Song, *Biomaterials*, 2012, **33**, 218-224.
17. C. A. Cezar, E. T. Roche, H. H. Vandenburgh, G. N. Duda, C. J. Walsh and D. J. Mooney, *Proc. Natl. Acad. Sci. U S A*, 2016, **113**, 1534-1539.
18. Y. S. Zhang and A. Khademhosseini, *Science*, 2017, **356**, 500-511.
19. T. Nonoyama and J. P. Gong, *Proc. Inst. Mech. Eng. H.*, 2015, **229**, 853-863.
20. Z. Gu, K. Huang, Y. Luo, L. Zhang, T. Kuang, Z. Chen and G. Liao, *Wiley Interdiscip. Rev. Nanomed. Nanobiotechnol.*, 2018, **10**, 1520-1534.
21. S. Azevedo, A. M. S. Costa, A. Andersen, I. S. Choi, H. Birkedal and J. F. Mano, *Adv. Mater.*, 2017, **29**, 1700759.
22. Z. Liu, Y. Faraj, X.-J. Ju, W. Wang, R. Xie and L.-Y. Chu, *J. Polym. Sci. Part B: Polym. Phys.*, 2018, **56**, 1306-1313.
23. G. Sharma, B. Thakur, M. Naushad, A. Kumar, F. J. Stadler, S. M. Alfadul and G. T. Mola, *Environ. Chem. Lett.*, 2017, **16**, 113-146.
24. N. Asadi, E. Alizadeh, R. Salehi, B. Khalandi, S. Davaran and A. Akbarzadeh, *Artif. Cells Nanomed. Biotechnol.*, 2018, **46**, 465-471.
25. Z. Wang, G. An, Y. Zhu, X. Liu, Y. Chen, H. Wu, Y. Wang, X. Shi and C. Mao, *Mater. Horiz.*, 2019, **6**, 733-742.
26. Z. Wang, Y. Ren, Y. Zhu, L. Hao, Y. Chen, G. An, H. Wu, X. Shi and C. Mao, *Angew. Chem. Int. Ed. Engl.*, 2018, **57**, 9008-9012.
27. H. Yan, Y. Chen, X.-D. Sun, L.-Y. Zhao, C.-X. Zhang, L. Bian, Y.-H. Yang, Y.-Z. Liu, J. Yuan, Y. Yao and Q. Wu, *J. Nanosci. Nanotechnol.*, 2017, **17**, 1983-1991.
28. H. Yan, W. Shang, X. Sun, L. Zhao, J. Wang, Z. Xiong, J. Yuan, R. Zhang, Q. Huang, K. Wang, B. Li, J. Tian, F. Kang and S.-S. Feng, *Adv. Funct. Mater.*, 2018, **28**, 1705710.
29. H. Yan, L. Zhao, W. Shang, Z. Liu, W. Xie, C. Qiang, Z. Xiong, R. Zhang, B. Li, X. Sun and F. Kang, *Nano Res.*, 2016, **10**, 704-717.
30. Y. Yang, X. Wang, F. Yang, H. Shen and D. Wu, *Adv. Mater.*, 2016, **28**, 7178-7184.
31. G. He, S. C, Y. Xu, Z. Miao, Y. Ma, H. Qian, Y. Lu, Z. Zha, *Mater. Horiz.,* 2019, **6**, 711--716.
32. J. Hu, Y. Chen, Y. Li, Z. Zhou and Y. Cheng, *Biomaterials*, 2017, **112**, 133-140.
33. M. A. Darabi, A. Khosrozadeh, R. Mbeleck, Y. Liu, Q. Chang, J. Jiang, J. Cai, Q. Wang, G. Luo and M. Xing, *Adv. Mater.*, 2017, **29**, 1700533.
34. F. Gao, Z. Xu, Q. Liang, B. Liu, H. Li, Y. Wu, Y. Zhang, Z. Lin, M. Wu, C. Ruan and W. Liu, *Adv. Funct. Mater.*, 2018, **28**, 1706644.
35. B. Grigoryan, S. Paulsen, D. Corbett, D. Sazer, C. Fortin, A. Zaita, P. Greenfield, N. Calafat, J. Gounley, A. Ta, F. Johansson, A. Randles, J. Rosenkrantz, J. Louis-Rosenberg, p. Galie, K. Stevens, J. Miller, *Science*, 2019, **364**, 458–464.
36. S. Liu and L. Li, *ACS Appl. Mater. Inter.*, 2017, **9**, 26429-26437.
37. L. Jiang, Y. Wang, Z. Liu, C. Ma, H. Yan, N. Xu, F. Gang, X. M. Wang, L. Zhao and X. Sun, Tissue Eng. Part B Rev., 2019, DOI: 10.1089/ten.TEB.2019.0100.

View Article Online
DOI: 10.1039/C9CC04241E

A strategy to improve the strength and self-healing properties of magnetic hydrogels while conferring its cytocompatibility and 3D printability.

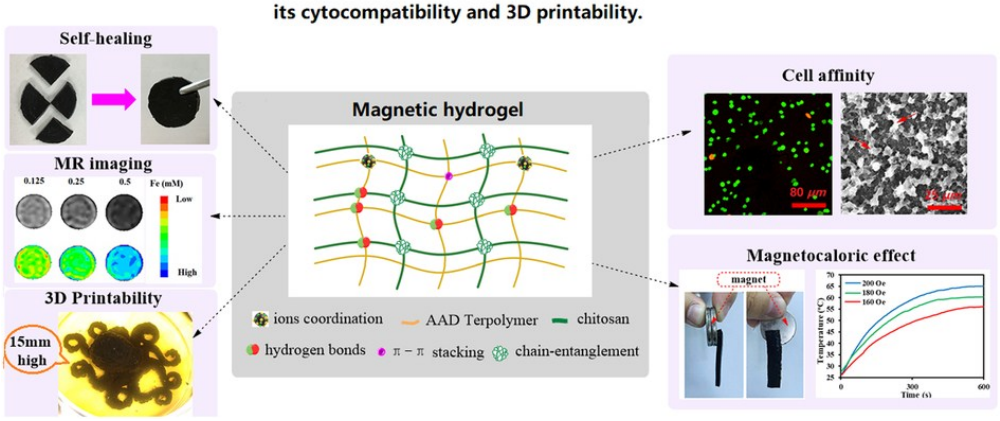

80x36mm (300 x 300 DPI)